Distributed Trajectory Optimization and Platooning of Vehicles to Guarantee Smooth Traffic Flow

Ge Guo, *Senior Member, IEEE*, Dongqi Yang, and Renyongkang Zhang

***Abstract*—This paper investigates a distributed trajectory optimization and control problem for a collection of vehicles with a quadratic spacing policy. A quadratic spacing policy is introduced based on the expected platoon speed to improve flexibility of speed planning and regulation. The trajectory optimization problem is solved using distributed convex optimization based on spacing errors minimization, resulting in an algorithm to provide the optimal trajectory for all following vehicles. Then, a PID-type sliding mode controller with a double high-power reaching law is presented for speed tracking control of each follower. The methodology can guarantee the internal stability, string stability and traffic flow stability with ignorable turbulence of spacing and speed, as demonstrated by numerical simulations.**

***Index Terms*—Distributed trajectory optimization, vehicular platoon, quadratic spacing policy, PID sliding mode control, string stability, traffic flow stability.**

I. Introduction

OVER the past few years, explosion of the number of vehicles has posed serious problems of traffic jam, air pollution, accidents and associated losses [1]–[3]. A promising approach to these problems is intelligent transportation systems, wherein vehicles on the road can drive in closely spaced convoys or platoons [4] to increase road throughput and reduce fuel consumption [5]–[7]. As vehicles in a platoon are dynamically coupled, any disturbances in the spacing or velocity may amplify when propagating backwards, known as unstable string [8], which can lead to traffic jams [9], [10] or even rear-ending accidents [4]. In order to achieve smooth and stable platooning, vehicles should cooperate with a certain communication topology, a good control algorithm and an appropriate spacing policy [11]. The most commonly used ones are the leader-predecessor following or predecessor following topology and the constant spacing (CS) or constant time-headway (CTH) spacing policy. A variety of platooning control algorithms are available, including model predictive control (MPC), sliding mode control, back-stepping control, and many others [12].

Platooning with a minimum cost of fuel or other costs is of great concern in many applications [4], [13]–[15]. Both centralized and decentralized/distributed methods are available along this direction. Centralized optimal control schemes, e.g., [4], [13], require a main controller (a roadside units or a leader vehicle) to coordinate all the vehicles, which is often impractical for use. Distributed MPC-based optimal platooning control methods can also been seen in in [14] for merging/splitting of vehicles and in [15] for a vehicular swarm.

Our concern is beyond optimal control of platoons with a given speed, instead, we are interested in a joint problem of vehicle speed planning and optimal tracking control. This important problem is studied in [4], which presents a framework for receding horizon speed planning and back-stepping platoon control. In the meanwhile, [13] gives an analytical solution to the same problem based on Pontryagin's minimum principle and sliding mode control. Being optimal in the sense of overall cost, however, these two results are often accompanied with turbulence of spacing errors in the transient state. As is well-known, inter-vehicle spacing errors are crucial for keeping the platoons compact [16], [17].

To address this issue, [18] proposes a distributed optimal platoon control method that minimizes a cost defined by inter-vehicle spacing errors. The result is built on a strict CS policy, which leaves little room for speed regulation to deal with the dynamic coupling among vehicles, resulting in degraded speed tracking and high communication cost [19], [20]. Besides, the simple sliding mode surface and reaching law used in [18] are subject to poor convergence and anti-chattering performance that is not good for string instability [21]–[23].

This paper revisits the problem in [18], aiming at improvements in at least two aspects. First, we introduce a quadratic spacing policy based on the leader speed (i.e., the expected platoon speed) to leave room for speed tracking, so as to ensure string stability and traffic flow stability. Second, a new PID-type sliding mode controller with a double high-power reaching law is presented, resulting in significantly improved platoon control performance and anti-chattering capacity. The main contributions are as follows:

1) By introducing a realistic team speed-dependent quadratic spacing policy, a distributed speed optimization method is derived for vehicles speed planning based on minimization of inter-vehicle spacing errors.

Manuscript received 17 May 2022; accepted 27 May 2022. Date of publication 31 May 2022; date of current version 23 January 2023. This work was supported in part by the National Natural Science Foundation of China under Grants 62173079 and U1808205, and in part by Science and Technology Program of Gansu Province under Grant 21ZD4GA028. *(Corresponding author: Ge Guo.)*

Ge Guo is with the State Key Laboratory of Synthetical Automation for Process Industries, Northeastern University, Shenyang 110819, China, and also with the School of Control Engineering, Northeastern University at Qinhuangdao, Qinhuangdao 066004, China (e-mail: geguo@yeah.net).

Dongqi Yang and Renyongkang Zhang are with the College of Information Science and Engineering, Northeastern University, Shenyang 110819, China (e-mail: ydq97@qq.com; zryk1998@163.com).

Color versions of one or more figures in this article are available at https://doi.org/10.1109/TIV.2022.3179293.

Digital Object Identifier 10.1109/TIV.2022.3179293

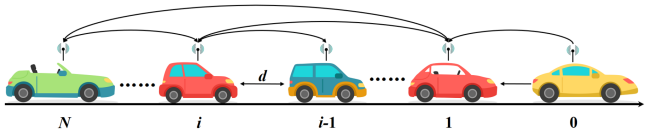

Fig. 1. Platoon communications and control system.

2) A PID-type sliding mode controller with a double high-power reaching law is presented, which is less sensitive to chattering of speed and spacing with a higher rate of convergence. In addition to performance and string stability, this method can also guarantee traffic flow stability, which is not addressed in [18].

Notations: Let $\mathbb{R}^n$ be the n-dimensional Euclidean space. Denote $1_N = [1, 1, \ldots, 1]^T \in \mathbb{R}^N$ and $0_N = [0, 0, \ldots, 0]^T \in \mathbb{R}^N$. $I_N \in \mathbb{R}^{N\times N}$ is the identity matrix of size $N \times N$. p-norm of vector x is denoted by $\|x\|_p$. For a matrix A, A^T is its the transpose matrix and $\lambda_{\min}(A)$ is the minimal eigenvalue of A. $diag\{\cdot\}$ is defined as the diagonal matrix. The matrix inequality $A > B$ ($A \geq B$) means that matrix $A - B$ is positive-define (semi definite). The Kronecker product is denoted by $\otimes$ and $sgn(\cdot)$ is the signum function.

II. Problem Description

Consider a collection of $N + 1$ vehicles driving as a platoon on the road (as shown Fig. 1), with the leader indexed by 0. Each follower can exchange information (e.g., position, velocity, acceleration) with its neighbors via the communication topology described as below.

A. The Platoon Topology

The communication among followers constitutes a directed graph $\mathcal{G}_N = (\mathcal{V}_N, \mathcal{E}_N)$, where the vertices set $\mathcal{V}_N = \{1, 2, \ldots, N\}$ represents vehicles and the edges set $\mathcal{E}_N \subseteq \mathcal{V}_N \times \mathcal{V}_N$ denotes communication link. Define the edge $\varepsilon_{ij} \triangleq (i, j) \in \mathcal{E}_N$, which means that there exists an information flow from vehicle j to vehicle i. The adjacency matrix of graph $\mathcal{G}_N$ is denoted by $A = [a_{ij}]_{N\times N}$, where $a_{ii} = 0$, $a_{ij} = 1$ if $\varepsilon_{ij} \in \mathcal{E}_N$, otherwise, $a_{ij} = 0$. The Laplacian matrix is defined as $\mathcal{L} = [l_{ij}]_{N\times N}$, where $l_{ij} = -a_{ij}$ for $i \neq j$ and $l_{ii} = \sum_{j=1}^{N} a_{ij}$. The incidence matrix is denoted by $D = [d_{ij}]_{N\times|\mathcal{E}_N|}$, where $d_{ij} = -1$ if the edge ε_j leaves node i, $d_{ij} = 1$ if it enters the node i, and $d_{ij} = 0$ otherwise. Note that $\mathcal{L} \triangleq DD^T$. A path is a sequence of connected edges and $\mathcal{G}_N$ is connected if there is a path between any two distinct nodes. We assume an undirected communication topology among the followers and the neighbor set of node i is

$$\mathbf{N}_i = \{j \in \mathcal{V}_N, (i, j) \in \mathcal{E}_N\}$$

The leader and all followers together form an augmented directed graph $\mathcal{G}_{N+1} = (\mathcal{V}_{N+1}, \mathcal{E}_{N+1})$ with vertices $\mathcal{V}_{N+1} = \{0, 1, \ldots, N\}$. Let $\mathcal{P} = diag\{p_1 p_2, \ldots, p_N\}$ be the pinning matrix, with $p_i = 1$ when vehicle i communicates with the leader, otherwise, $p_i = 0$. Note that, for $\mathcal{G}_{N+1}$, $\mathcal{L} + \mathcal{P} \triangleq \bar{D}\bar{D}^T$, where $\bar{D} = [d_{ij}]_{N\times|\mathcal{E}_{N+1}|}$, is the incidence matrix.

The set indicating if the leader is reachable for vehicle i is denoted by

$$\mathbf{P}_i = \begin{cases} \emptyset & if \quad p_i = 0 \\ \{0\} & if \quad p_i = 1 \end{cases} \tag{1}$$

where $\emptyset$ is the empty set. Then, the set of neighbors of vehicle i is $\mathbf{I}_i = \mathbf{N}_i \cup \mathbf{P}_i$

Assumption 1: $\mathcal{G}_{N+1} = (\mathcal{V}_{N+1}, \mathcal{E}_{N+1})$ representing the communication topology among the leader and followers has at least one spanning tree rooted in the leader.

Lemma 1: If $\mathcal{L}$ is the Laplace matrix of an undirected connected graph, then $\lambda_{\min}(\mathcal{L}) = 0$ with $\mathbf{1}_N$ being the associated eigenvector. For graphs satisfying Assumption 1, $\lambda_{\min}(\mathcal{L}) = 0$ is a simple eigenvalue, and $\lambda_{\min}(\mathcal{L} + \mathcal{P}) \geq 0$ [24].

B. Vehicle Longitudinal Modeling and the Spacing Policy

Let $x_i(t)$, $v_i(t)$ and $a_i(t)$ be, respectively, the position, velocity and acceleration of vehicle $i = 0, 1, 2, ..., N$. Assume that the leader executes a constant team speed trajectory, namely, $a_0 = 0$, $x_0 = v_0 t$. For the follower vehicles, we consider the following longitudinal dynamics

$$\begin{cases} \dot{x}_i(t) = v_i(t) \\ \dot{v}_i(t) = a_i(t) \\ \dot{a}_i(t) = -\xi_i a_i(t) + \xi_i u_{i2}(t) \end{cases} \tag{2}$$

where $\xi_i = 1/\iota_i$ and u_{i2} is the control input. ι_i is the time constant in the drivetrain system of vehicle i.

Let $d_{i,i-1}(t) > 0$ be the desired distance between vehicles i and $i - 1$. We introduce the following quadratic spacing strategy, which is based on the leader speed (i.e., the expected platoon speed):

$$d_{i,i-1}(t) = hv_0^2(t) + cv_0(t) + l_i \tag{3}$$

where $h > 0, c$ are coefficients, $l_i > 0$ denotes the expected inter-vehicle spacing when stationary, wherein the vehicle length L_i is considered. These parameters can be designed to ensure traffic flow stability, as will be given later.

C. The Objective

Consider the optimization problem as below:

$$\min_{x_i(t)} J(t) = \sum_{i=1}^{N} \delta_i^2(t) \tag{4a}$$

$$s.t. \begin{cases} \lim\limits_{t\to\infty} |v_i(t) - v_0(t)| = 0 \\ \lim\limits_{t\to\infty} |\delta_i(t)| = 0 \end{cases} \tag{4b}$$

where $\delta_i(t)$ is the spacing error for follower vehicle i, which is defined as

$$\delta_i(t) = x_i(t) - x_{i-1}(t) + d_{i,i-1}(t) + L_{i-1} \tag{5}$$

Aiming to solve problem (4a) and (4b), a distributed speed trajectory optimization and platoon control framework should

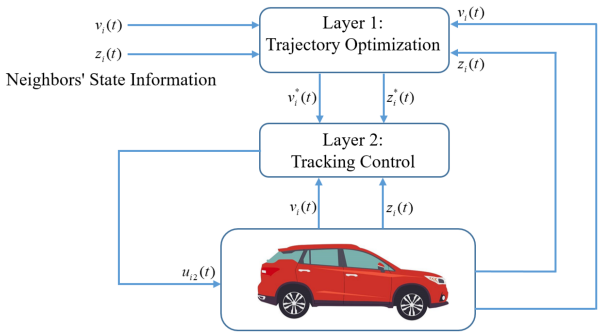

Fig. 2. The proposed two-layer control structure for platoon.

be designed and the controller of all the followers should meet the following criteria:

1) *Internal stability [8]:* The speed and acceleration of all followers can track the leader with convergent spacing errors.
2) *String stability [8]:* $|\delta_N(s)| \leq |\delta_{N-1}(s)| \leq \cdots \leq |\delta_1(s)|$, or, equivalently, the error transfer function $G_i(s) = \delta_{i+1}(s)/\delta_i(s)$ satisfies $|G_i(s)| \leq 1$, where $\delta_i(s)$ is the Laplace transform of $\delta_i(t)$.
3) *Traffic flow stability [23], [25]:* The gradient inequality $\partial Q/\partial P > 0$ should be guaranteed, where Q and P are the flow rate and density of road traffic, respectively.

In order to achieve the above objectives, a two-layered framework is proposed (see Fig. 2), with trajectory optimization and tracking control in different layers.

Remark 1: The optimal control method in [4], [13] is based on CS policy and is aimed at saving fuel and time, but pays little attention to smoothness and stability of traffic flow. Unlike their centralized methods, we give a fully distributed framework based a quadratic spacing policy to strengthen traffic flow stability with decreased cost of calculation and communication.

III. Distributed Trajectory Optimization

Let the reference trajectories of the position and speed for the following vehicle i be given by

$$\begin{cases} \dot{x}_i^*(t) = v_i^*(t) \\ \dot{v}_i^*(t) = u_{i1}(t) \end{cases} \tag{6}$$

We aim to find a controller $u_{i1}(t)$ to generate the reference trajectories $x_i^*(t)$ and $v_i^*(t)$ that solves the distributed optimization problem in (4a) and (4b). To this end, introduce the following reference position errors and reference velocity errors,

$$\begin{cases} \hat{x}_i^*(t) = x_i^*(t) - x_0(t) + d_{i,0}(t) \\ \hat{v}_i^*(t) = v_i^*(t) - v_0(t) \end{cases} \tag{7}$$

by which we can have that

$$\begin{cases} \hat{x}_i^*(t) - \hat{x}_j^*(t) = x_i^*(t) - x_j^*(t) + d_{i,j}(t) \\ \hat{v}_i^*(t) - \hat{v}_j^*(t) = v_i^*(t) - v_j^*(t) \end{cases} \tag{8}$$

Taking the time derivative of (7), we can obtain that

$$\begin{cases} \dot{\hat{x}}_i^*(t) = \hat{v}_i^*(t) + d(\sum_{i=1}^N (hv_0^2 + cv_0 + l_i))/dt \\ \hat{v}_i^*(t) = v_i^*(t) - v_0(t) \end{cases} \tag{9}$$

by which and (6), we can have

$$\begin{cases} \dot{\hat{x}}_i^*(t) = \hat{v}_i^*(t) \\ \dot{\hat{v}}_i^*(t) = u_{i1}(t) \end{cases} \tag{10}$$

Now, according to (7) and (8), the (4a) and (4b) can be equivalently written as follows

$$\min_{\hat{x}_i^*(t)} J = \sum_{i=1}^{N} [\hat{x}_i^*(t) - \hat{x}_{i-1}^*(t)]^2 \tag{11a}$$

$$s.t. \begin{cases} \lim\limits_{t\to\infty} \hat{x}_i^*(t) = \hat{x}_j^*(t) \\ \lim\limits_{t\to\infty} \hat{v}_i^*(t) = \hat{v}_j^*(t) \end{cases} \tag{11b}$$

Based on the above discussions, the problem now becomes as designing $u_{i1}(t)$ so that the optimization problem in (11) is solved with (10). To this end, we have the following result.

Theorem 1: For a vehicular platoon with topologies satisfying Assumption 1, if $\frac{\rho}{\tau\varsigma} < \lambda_{\min}(L + \mathcal{P})$ holds for positive parameters η, τ, ρ and ς, then the controller that solves the optimization problem in (4a) and (4b) is given below, which generates the reference trajectory $x_i^*(t)$ and $v_i^*(t)$ for the group of vehicles,

$$\begin{aligned} u_{i1}(t) = & -\sum_{j\in I_i} (\eta(x_i(t) - x_j(t) + d_{i,j}(t)) + \tau(v_i(t) - v_j(t))) \\ & - \sum_{j\in I_i} \{\chi_{ij}(t) sgn(\rho(x_i(t) - x_j(t) + d_{i,j}(t)) \\ & + \varsigma(v_i(t) - v_j(t)))\} + \psi_i(t) \end{aligned} \tag{12}$$

where the controller gain $\chi_{ij}(t) = \chi_{ji}(t) \geq 0$ and internal signal $\psi_i(t)$ are given by

$$\dot{\chi}_{ij}(t) = |\rho(x_i(t) - x_j(t) + d_{i,j}(t)) + \varsigma(v_i(t) - v_j(t))| \tag{13}$$

$$\psi_i(t) = -2(x_i(t) - x_j(t) + d_{i,j}(t)) - (v_i(t) - v_j(t)) \tag{14}$$

Proof: See the Appendix. ■

Remark 2: Similar to [18], the proposed quadratic spacing policy (3) can transform the reference platoon dynamics into a standard double integrator by introducing reference position and velocity errors. Using this spacing policy, the resulted method can ensure traffic flow stability within a critical traffic density (as shown latter).

IV. Tracking Controller Design

This section, we design the sliding mode controller by introducing an improved PID-type sliding mode surface, which is valued by its exceptional properties in tracking and eliminating steady-state spacing errors. The controller $u_{i2}(t)$ is designed to track the reference position $x_i^*(t)$ and speed $x_i^*(t)$, which guarantees the individual stability, string stability and traffic flow stability.

A. Controller and Internal Stability Analysis

In order to track the reference position and velocity signals from the first layer, the tracking errors are first defined as follows

$$\begin{cases} \tilde{x}_i(t) = x_i(t) - x_i^*(t) \\ \tilde{v}_i(t) = v_i(t) - v_i^*(t) \end{cases} \tag{15}$$

Define the total tracking errors

$$e_i(t) = \tilde{x}_i(t) + \tilde{v}_i(t). \tag{16}$$

It follows that

$$\begin{cases} \dot{e}_i(t) = \dot{\tilde{x}}_i(t) + \dot{\tilde{v}}_i(t) = \tilde{v}_i(t) + \tilde{a}_i(t) \\ \ddot{e}_i(t) = \dot{\tilde{v}}_i(t) + \dot{\tilde{a}}_i(t) = a_i(t) - u_{i1}(t) + \dot{a}_i(t) - \dot{u}_{i1}(t) \end{cases} \tag{17}$$

where $\tilde{a}_i(t) = a_i(t) - u_{i1}(t)$.

Introduce the following PID-type sliding mode surface:

$$s_i(t) = k_p e_i(t) + k_i \int_0^t {e_i}^{q/p}(\tau)d\tau + k_d \dot{e}_i(t) \tag{18}$$

where k_p, k_i and k_d are positive real numbers, p and q denote the odd positive integer values with $q < p$. The results of tracking controller design are presented below, expressed by the following theorem.

Theorem 2: If the controller $u_{i2}(t)$ of each follower is designed as below, then the sliding mode surface $s_i(t)$ can converge to zero complying with reaching law (21):

$$\begin{aligned} u_{i2}(t) = & -\frac{1}{\xi_i}a_i(t) + a_i(t) - \frac{k_p}{\xi_i k_d}\dot{e}_i(t) - \frac{k_i}{\xi_i k_d}{e_i}^{q/p}(t) \\ & - \frac{K_1}{\xi_i k_d}{s_i}^{\alpha}(t) - \frac{K_2}{\xi_i k_d}{s_i}^{\beta}(t) \end{aligned} \tag{19}$$

where ξ_i is determined by the engine time constant, K_1 and K_2 are both positive real numbers, and $\alpha, \beta > 0$ are odd numbers.

Proof: The time derivative of the sliding mode surface $s_i(t)$ is give as below

$$\dot{s}_i(t) = k_p\dot{e}_i(t) + k_i{e_i}^{q/p}(t) + k_d(a_i(t) - \xi_i a_i(t) + \xi_i u_{i2}(t)) \tag{20}$$

Substituting (19) into (20), we obtain

$$\dot{s}_i(t) = -K_1{s_i}^{\alpha}(t) - K_2{s_i}^{\beta}(t) \tag{21}$$

Choose the Lyapunov function as below

$$V_0(t) = \frac{1}{2}{s_i}^2(t) \tag{22}$$

whose time derivative is

$$\begin{aligned} \dot{V}_0(t) &= s_i(t)\dot{s}_i(t) \\ &= -K_1{s_i}^{\alpha+1}(t) - K_2{s_i}^{\beta+1}(t) \\ &\le 0 \end{aligned} \tag{23}$$

which implies that sliding mode surface $s_i(t)$ converges to the origin. Here, (21) is the chosen reaching law to ensure the convergence speed and smoothness of the designed controller.

According to (18), when the sliding mode surface is reached, we have the following tracking error dynamics

$$\dot{e}_i(t) = -\frac{k_p}{k_d}e_i(t) - \frac{k_i}{k_d}\int_0^t {e_i}^{q/p}(\nu)d\nu \tag{24}$$

which is asymptotically convergent as shown by the following result.

Theorem 3: For mutually odd parameters p and q, if $0 < q < p$, then position tracking errors $\tilde{x}_i(t)$ and velocity tracking errors $\tilde{v}_i(t)$ can converge to zero asymptotically on the sliding mode surface with the sliding mode controller in (19).

Proof: For the tracking error system (24), define the following Lyapunov function

$$V_1(t) = \frac{1}{2}{e_i}^2(t) \tag{25}$$

whose time derivative of $V_1(t)$ along system (24) is

$$\dot{V}_1(t) = e_i(t)\left(-\frac{k_p}{k_d}e_i(t) - \frac{k_i}{k_d}\int_0^t {e_i}^{q/p}(\nu)d\nu\right) \tag{26}$$

Since p and q are mutually odd with $0 < q < p$, we have that

$$\dot{V}_1(t) = -\frac{k_p}{k_d}{e_i}^2(t) - \frac{k_i}{k_d}\int_0^t \left({e_i}^2(\nu)\right)^{\frac{q/p+1}{2}}d\nu \le 0 \tag{27}$$

which means that the tracking errors $e_i(t)$ will converge asymptotically to zero, i.e., $\tilde{x}_i(t) + \tilde{v}_i(t) \to 0$. Thus, $\dot{\tilde{x}}_i(t) = \tilde{v}_i(t) = -\tilde{x}_i(t)$, which is asymptotically stable. So, the position tracking errors $\tilde{x}_i(t)$ and the velocity tracking errors $\tilde{v}_i(t)$ can be stabilized asymptotically. ■

Remark 3: In comparison with the methods in [18] and [13], by introducing the term with fractional-order q/p to reduce integral saturation, the PID-type sliding mode controller proposed in this paper has better performance in convergence speed and control accuracy, as well as better robustness and anti-disturbance ability.

B. String Stability

For vehicles platoon with a constant pacesetter's velocity, $u_{i1}(t) = 0$ should be known as well as $\tilde{x}_0(t) = 0$, $\tilde{v}_0(t) = 0$ and $e_0 = 0$ hold.

By definition, the inter-vehicle spacing errors $\delta_i(t)$ (5) satisfies that

$$\dddot{\delta}_i(t) = \dddot{x}_i(t) - \dddot{x}_{i-1}(t) = \dot{a}_i(t) - \dot{a}_{i-1}(t) \tag{28}$$

According to (2) and the designed controller $u_{i2}(t)$, we have that

$$\dot{a}_i(t) = -a_i(t) - \frac{k_p}{k_d}\dot{e}_i(t) - \frac{k_i}{k_d}{e_i}^{q/p}(t) \tag{29}$$

which, together with (28), leads to the following spacing error dynamics

$$\begin{aligned} \dddot{\delta}_i(t) &= \dot{a}_i(t) - \dot{a}_{i-1}(t) \\ &= \left(-a_i(t) - \frac{k_p}{k_d}\dot{e}_i(t) - \frac{k_i}{k_d}{e_i}^{q/p}(t)\right) \\ &\quad - \left(-a_{i-1}(t) - \frac{k_p}{k_d}\dot{e}_{i-1}(t) - \frac{k_i}{k_d}{e_{i-1}}^{q/p}(t)\right) \end{aligned} \tag{30}$$

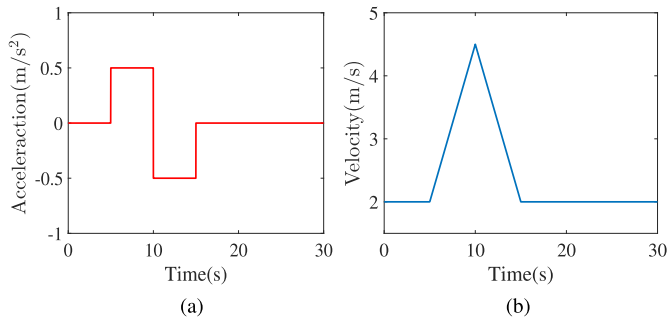

Fig. 3. Desired profile of the leader's acceleration (a) and velocity (b).

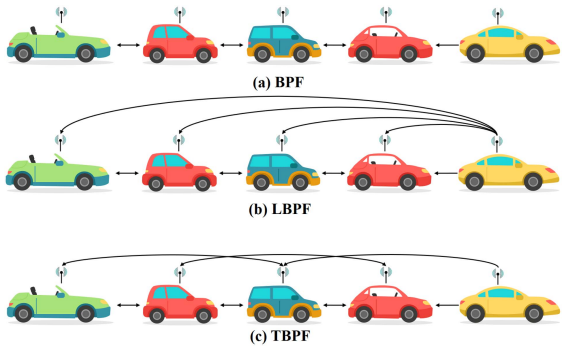

Fig. 4. Three communication topologies for platoons.

On the sliding mode surface, one can get $\dot{s}_i(t) = 0$. So, $k_p\dot{e}_i(t) + k_i {e_i}^{q/p}(t) + k_d\ddot{e}_i(t) = 0$, namely

$$ {e_i}^{q/p}(t) = -\frac{k_p}{k_i}\dot{e}_i(t) - \frac{k_d}{k_i}\ddot{e}_i(t) \tag{31}$$

Thus, (30) can be rewritten as

$$\begin{aligned}\dddot{\delta}_i(t) = &-(a_i(t) - a_{i-1}(t)) - \frac{k_p}{k_d}(\dot{e}_i(t) - \dot{e}_{i-1}(t)) \\ &+ \frac{k_p}{k_d}(e_i(t) - e_{i-1}(t)) + \ddot{e}_i(t) - \ddot{e}_{i-1}(t)\end{aligned} \tag{32}$$

By definitions given earlier, it follows that,

$$\ddot{\delta}_i(t) - \delta_i(t) = \ddot{d}(t) - d(t) - \frac{k_d}{k_p}\ddot{d}(t) - \frac{k_d}{k_p}\dddot{d}(t)$$

which, by Laplace transform, is equivalent to

$$\delta_i(s) = \frac{-\frac{k_p}{k_d}\cdot s^3 d_{i,i-1}(s) + (1-\frac{k_p}{k_d})\cdot s^2 d_{i,i-1}(s) - d_{i,i-1}(s)}{s^2 - 1}$$

where s is a complex variable. Therefore, we can have the following transfer function for $i = 1, 2, \ldots, N$

$$\begin{aligned}G_i(s) &= \frac{\delta_{i+1}(s)}{\delta_i(s)} \\ &= \frac{-\frac{k_p}{k_d}\cdot s^3 d_{i+1,i}(s) + (1-\frac{k_p}{k_d})\cdot s^2 d_{i+1,i}(s) - d_{i+1,i}(s)}{-\frac{k_p}{k_d}\cdot s^3 d_{i,i-1}(s) + (1-\frac{k_p}{k_d})\cdot s^2 d_{i,i-1}(s) - d_{i,i-1}(s)}\end{aligned}$$

According to the spacing policy, the inter-vehicle spacing in the platoon is equal in the s domain, i.e., $d_{i,i-1}(s) = d_{i+1,i}(s)$. So we have that, $G_i(s) = 1$ for all vehicles, namely, string stability can be guaranteed.

C. Traffic Flow Stability

The condition and critical traffic density for traffic flow stability are given below.

Theorem 4: For the vehicular platoon system in (2), if $h \geq c^2/4l$ and $-2\sqrt{h(l+L)} \leq c \leq 0$, then the quadratic spacing policy (3) and the control method can guarantee traffic flow stability. Furthermore, the critical traffic density is given by

$$P_{\lim} = \frac{h}{c\sqrt{h(l+L)}+2h(l+L)} - \frac{h}{c\sqrt{h(l+L)}-2h(l+L)}.$$

Proof: If $h \geq c^2/4l$ holds, it follows that $d_{i,i-1}(t) > 0$ for $\forall v_0(t) > 0$. In the steady-state of road traffic, it is natural that the speed and separation of each vehicle are identical, i.e., $d_{i,i-1}(t) = d_{steady}(t)$ and $v_i(t) = v(t)$, for all i. Hence, according to [25], one can have the traffic density in steady-state distance

$$d_{steady}(t) = hv^2(t) + cv(t) + l + L \tag{33}$$

the steady-state traffic density

$$P = \frac{1}{d_{steady}} = \frac{1}{hv^2(t) + cv(t) + l + L} \tag{34}$$

According to the flow and density formula $Q = Pv$ and Equation (34), it can be obtained the following traffic flow rate

$$Q(P) = P\left(-\frac{c}{2h} + \frac{\sqrt{c^2 - 4h(l+L-\frac{1}{P})}}{2h}\right)$$

Taking partial derivatives can lead to

$$\begin{aligned}\frac{\partial Q}{\partial P} = &-\frac{c}{2h} + \frac{\sqrt{c^2 - 4h(l+L-\frac{1}{P})}}{2h} \\ &- \frac{1}{P\sqrt{c^2 - 4h(l+L-\frac{1}{P})}}\end{aligned}$$

From $\frac{\partial Q}{\partial P} = 0$, we can get the upper limit of traffic flow density $P_{\lim}$ as

$$P_{\lim} = \frac{h}{c\sqrt{h(l+L)} + 2h(l+L)} - \frac{h}{c\sqrt{h(l+L)} - 2h(l+L)} \tag{35}$$

Note that $P_{\lim} \geq 0$ for $-2\sqrt{h(l+L)} \leq c \leq 0$. ■

Remark 4: Unlike the result in [18], the presented method can guarantee traffic flow stability given that the traffic density is below a critical value, besides individual vehicle stability and string stability, by introducing a quadratic spacing policy.

V. Numerical Simulations

This section shows the implementation and performance of the presented platoon control method in numerical simulations. Consider a platoon of five vehicles, wherein the leader is denoted as 0 and the followers are 1 to 4 whose parameters are shown in Table I.

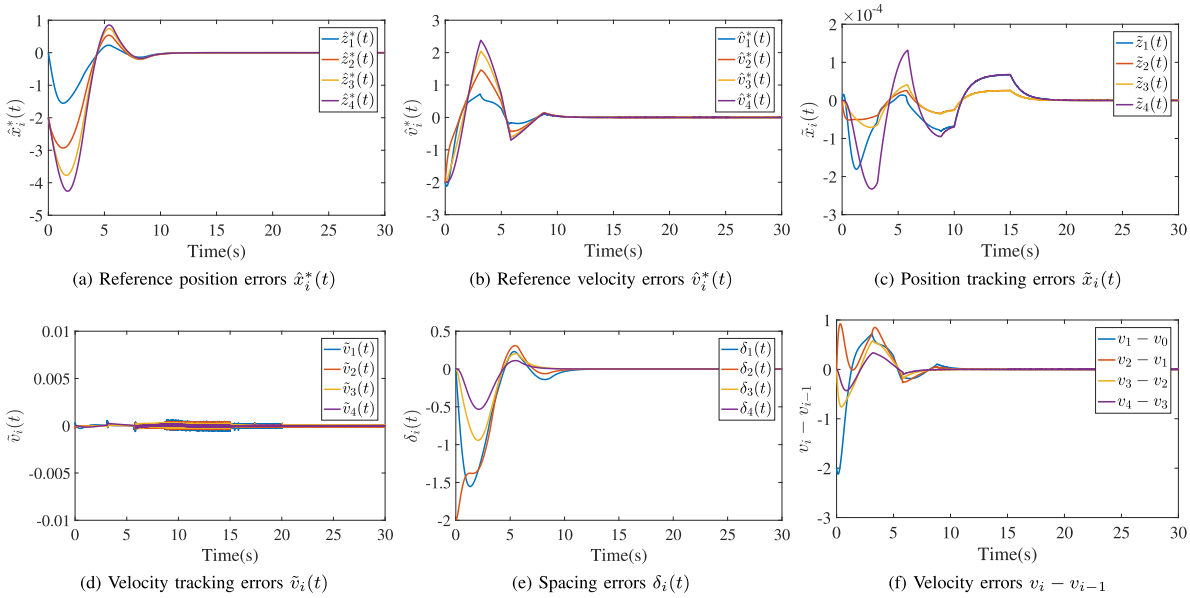

(a) Reference position errors $\hat{x}_i^*(t)$ (b) Reference velocity errors $\hat{v}_i^*(t)$ (c) Position tracking errors $\tilde{x}_i(t)$

(d) Velocity tracking errors $\tilde{v}_i(t)$ (e) Spacing errors $\delta_i(t)$ (f) Velocity errors $v_i - v_{i-1}$

Fig. 5. Simulation results of the platoon with the devised control framework under BPF.

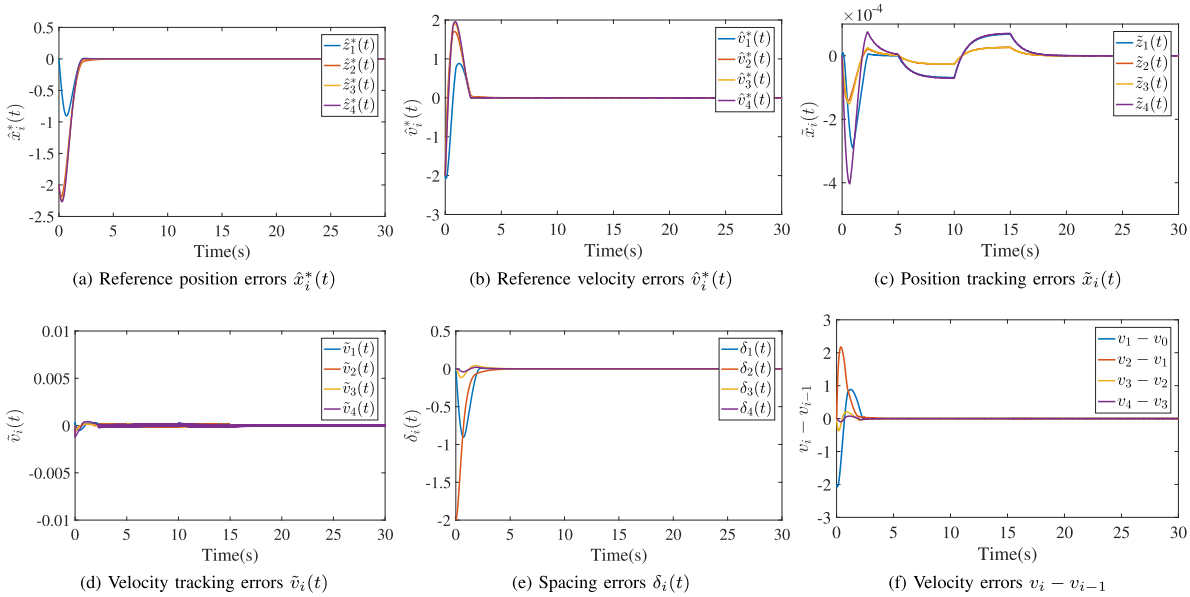

(a) Reference position errors $\hat{x}_i^*(t)$ (b) Reference velocity errors $\hat{v}_i^*(t)$ (c) Position tracking errors $\tilde{x}_i(t)$

(d) Velocity tracking errors $\tilde{v}_i(t)$ (e) Spacing errors $\delta_i(t)$ (f) Velocity errors $v_i - v_{i-1}$

Fig. 6. Simulation results of the platoon under LBPF with the devised control framework.

TABLE I
PHYSICAL PARAMETERS USED IN THE EXPERIMENTS

Vehicle Index	1	2	3	4
$\xi_i(s^{-1})$	0. 50	0. 25	0. 60	0. 35
$L_i(m)$	5.0	4.6	4.9	4.7

A. *Effectiveness of the Presented Method*

In the simulations, the initial positions of the five vehicles are $x(0) = [0, -5, -12, -17, -22]$ m. The velocity and acceleration of the leader are given in Fig. 3, and the followers all have zero initial velocities with non-zero initial spacing errors. Communication topologies considered in the simulations include Bidirectional-predecessor Following (BPF), Leader-bidirectional-predecessor Following (LBPF) and Two-bidirectional-predecessor Following (TBPF) (see Fig. 4), all of which satisfy Assumption 1. According to Theorem 1, 2 and 3, the parameters of controller $u_{i1}(t)$ and tracking controller $u_{i2}(t)$ are listed in Table II.

The trajectory optimization and tracking control results of these vehicles under topologies BPF, LBPF and TBPF are given

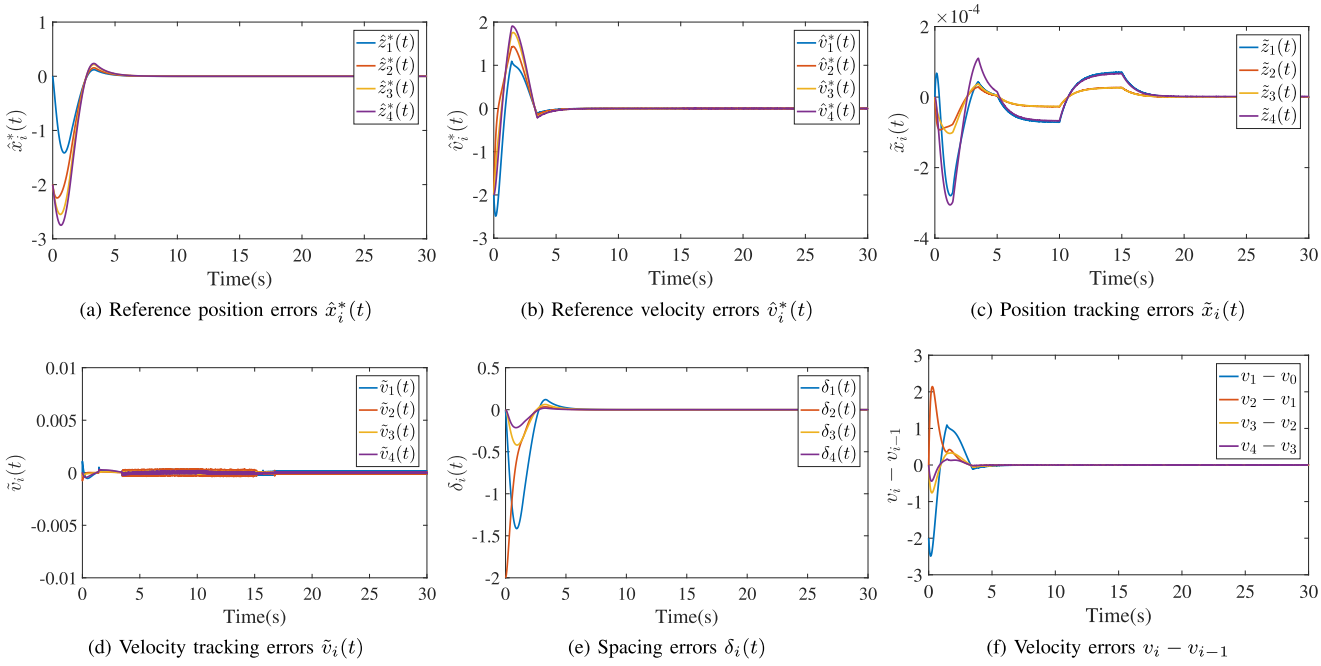

(a) Reference position errors $\hat{x}_i^*(t)$ (b) Reference velocity errors $\hat{v}_i^*(t)$ (c) Position tracking errors $\tilde{x}_i(t)$

(d) Velocity tracking errors $\tilde{v}_i(t)$ (e) Spacing errors $\delta_i(t)$ (f) Velocity errors $v_i - v_{i-1}$

Fig. 7. Simulation results of the platoon control system with the devised control framework under TBPF.

TABLE II
PARAMETERS USED IN THE DEVISED CONTROL STRUCTURE

Parameter Names	Simulation Values	Parameter Names	Simulation Values
η	0.5	q	3
τ	0.5	α	5
ρ	0.5	β	7
ς	0.5	K_1	5
p	5	K_2	40

in Fig. 5–Fig. 7, respectively. In these figures, (a) and (b) show that the reference trajectory (position and velocity) of all vehicles can achieve consensus with that of the leader; (c) and (d) means that, with the method in this paper, all vehicles can track their reference trajectory; (e) and (f) show that the spacing errors and velocity errors between neighboring vehicles can both converge to zero. The real-time position of these vehicles under three topologies are shown in Fig. 8. From these results it is clearly seen that string stability and smooth traffic flow are well guaranteed.

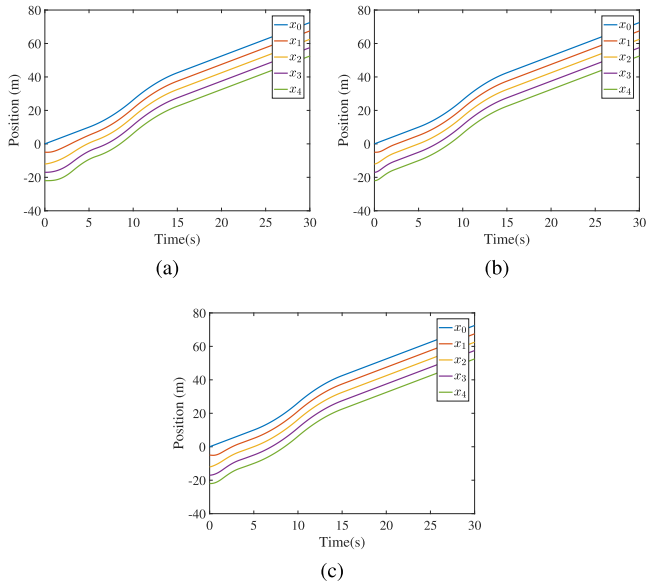

(a) (b)

(c)

Fig. 8. Time-position diagram of the five-vehicles platoon under BPF (a), LBPF (b) and TBPF (c) communication topologies.

B. Performance Comparisons

The proposed method is compared with two benchmark methods in [26] and Wen *et al.* [18], based on the following performance measures

$$\begin{cases} J_1(t) = \lim\limits_{T\to\infty} \int_0^T \sum\limits_{i=1}^{4} \delta_i^2(t)dt \\ J_2(t) = \lim\limits_{T\to\infty} \int_0^T \sum\limits_{i=1}^{4} \tilde{x}_i^2(t)dt \end{cases} \tag{36}$$

where, $J_1(t)$ is the overall spacing errors, and $J_2(t)$ represents the tracking performance.

Fig. 9 shows the actual velocity, the spacing errors and velocity errors of the platoon under LBPF communication topology. It can be seen that the inter-vehicle spacing errors and speed tracking errors of the proposed method are smaller and converging faster without obvious chattering. The corresponding performance measures are shown in Table III.

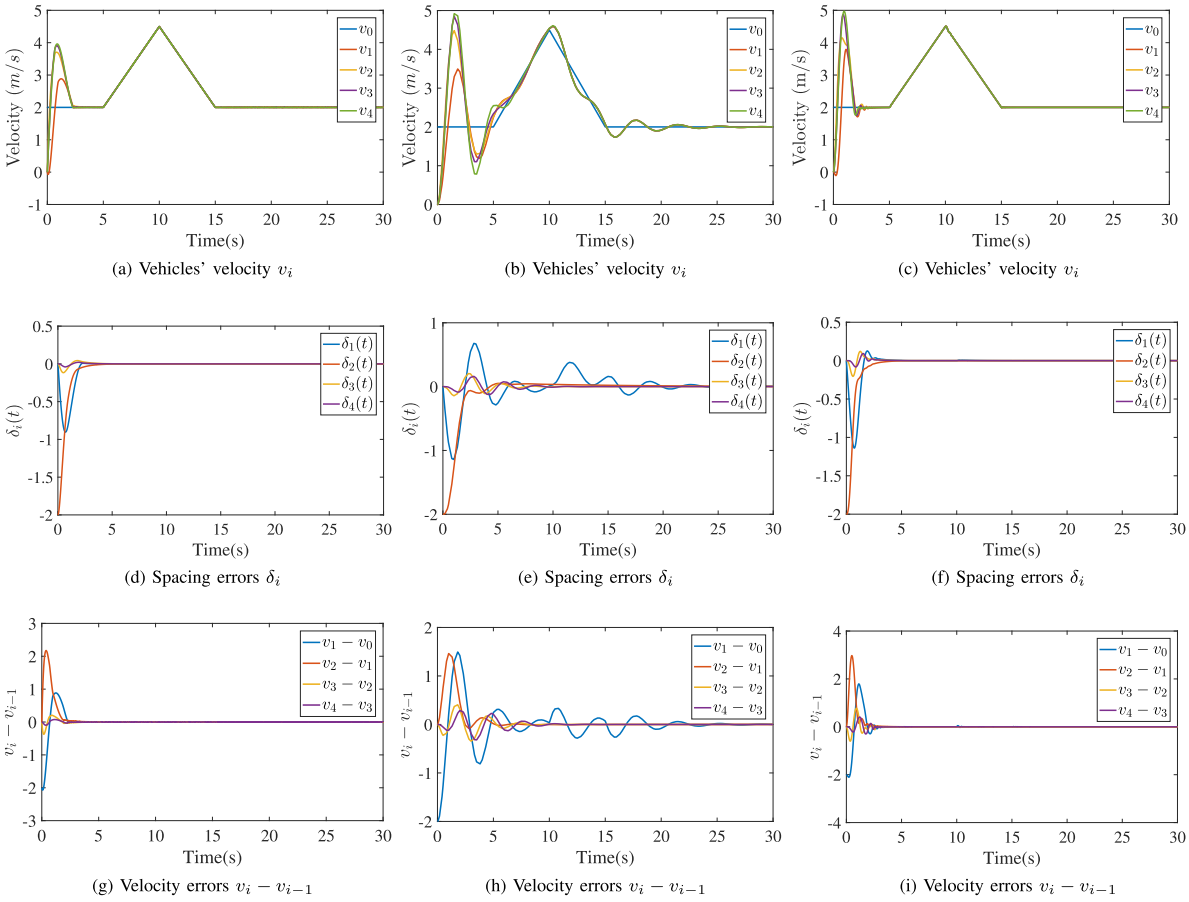

(a) Vehicles' velocity v_i (b) Vehicles' velocity v_i (c) Vehicles' velocity v_i

(d) Spacing errors δ_i (e) Spacing errors δ_i (f) Spacing errors δ_i

(g) Velocity errors $v_i - v_{i-1}$ (h) Velocity errors $v_i - v_{i-1}$ (i) Velocity errors $v_i - v_{i-1}$

Fig. 9. Comparisons of platoon control performance under LBPF among the proposed method (left), [26] (middle) and [18] (right).

TABLE III
PERFORMANCE MEASURES FOR THE PLATOON WITH DIFFERENT CONTROLLERS UNDER LBPF

Controller	Proposed	Fiengo *et al.* [26]	Wen *et al.* [18]
$J_1(t)$	2.422	5.914	2.702
$J_2(t)$	3.095×10^{-7}	-	0.762
Settling Time (s)	3.783	18.810	4.978

Then, we compare the performance of our method with that of [18] and [26] in the existence of jerks in the leader acceleration

$$a_{jerk}(t) = a_0(t) + \sigma(t) \tag{37}$$

where $a_0(t)$ denotes the original leader acceleration and $\sigma(t)$ indicates the jerk, which takes arbitrary values in [-0.15, 0.15]. The acceleration and velocity of the leader in this case are shown in Fig. 10.

The performance comparisons are shown in Fig. 11, from which it can be seen that the method in [18] cannot deal with the acceleration jerk. The performance of our method is clearly much better, with faster convergent tracking errors an no oscillations. The performance measures under LBPF communication topology are given in Table IV, which show the clear advantage of our method. Fig. 11 depicts the inter-spacing errors and velocity errors between neighbors.

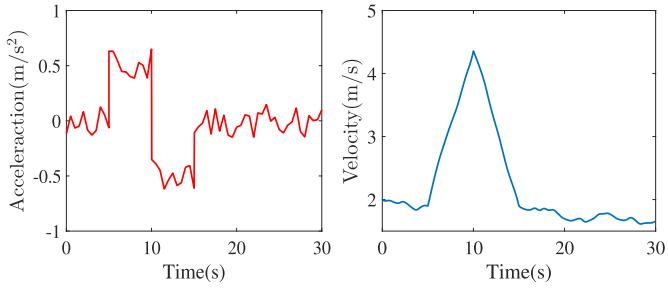

(a) (b)

Fig. 10. Acceleration (a) and velocity (b) of the leader with random jerk.

TABLE IV
PERFORMANCE MEASURES FOR THE PLATOON WITH RANDOM JERK USING DIFFERENT CONTROLLERS UNDER LBPF

Controller	Proposed	Fiengo *et al.* [26]	Wen *et al.* [18]
$J_1(t)$	2.410	5.911	2.709
$J_2(t)$	3.079×10^{-7}	-	0.762
Settling Time (s)	4.647	27.82	5.071

Finally, a comparison with the centralized control scheme [27] is provided to demonstrate the advantages of the distributed framework in larger size platoon. Fig. 12 depicts the position

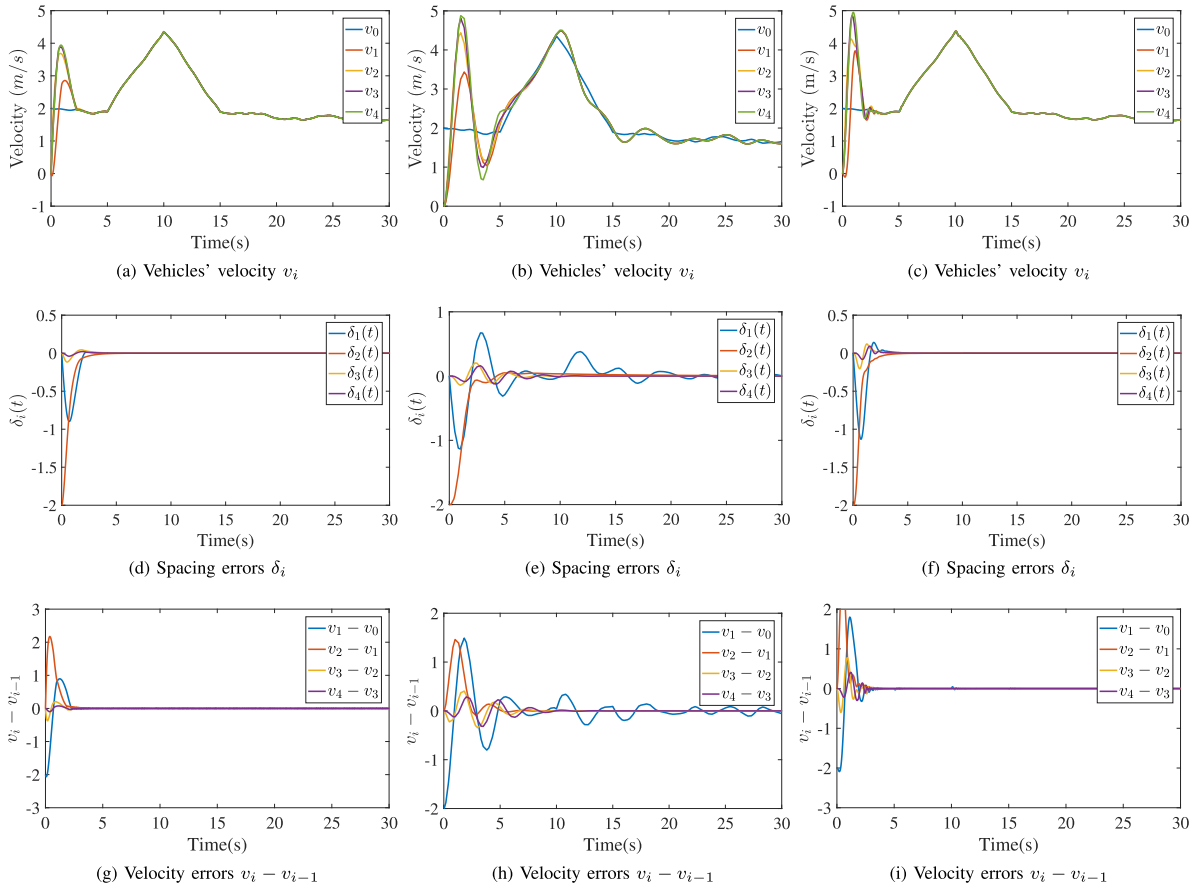

(a) Vehicles' velocity v_i (b) Vehicles' velocity v_i (c) Vehicles' velocity v_i

(d) Spacing errors δ_i (e) Spacing errors δ_i (f) Spacing errors δ_i

(g) Velocity errors $v_i - v_{i-1}$ (h) Velocity errors $v_i - v_{i-1}$ (i) Velocity errors $v_i - v_{i-1}$

Fig. 11. Comparisons of platoon control performance with random jerk under LBPF among the proposed method (left), [26] (middle) and [18] (right).

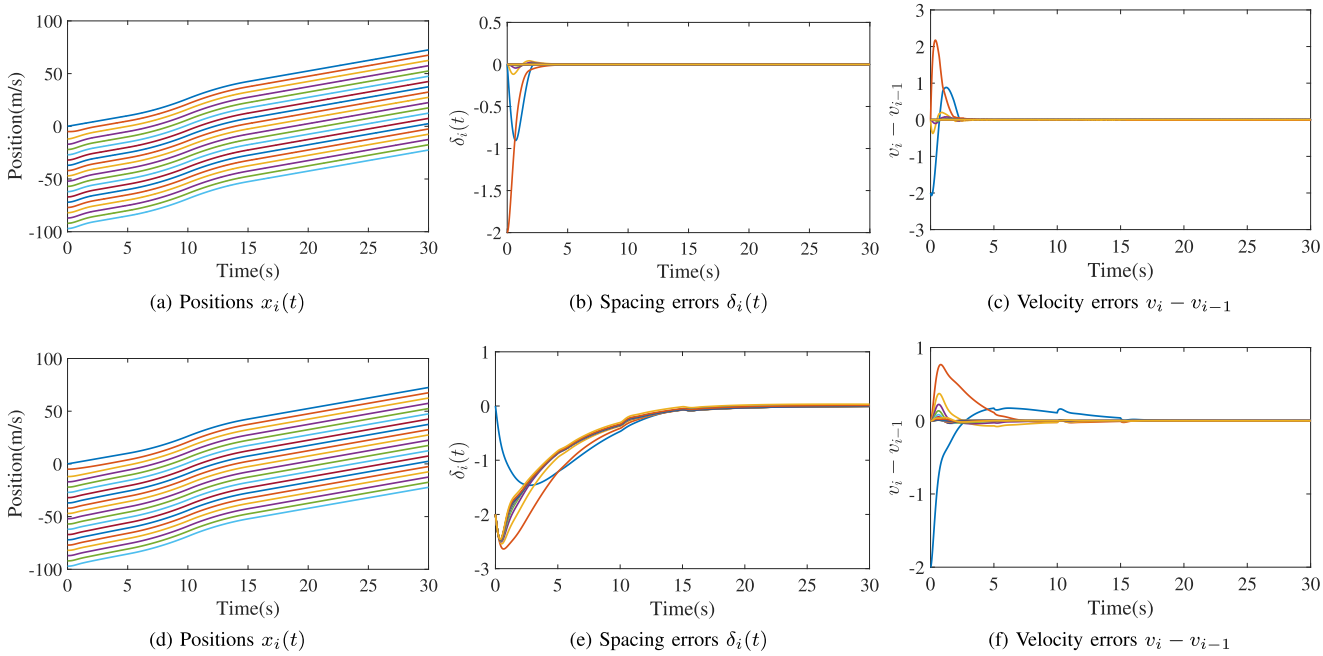

(a) Positions $x_i(t)$ (b) Spacing errors $\delta_i(t)$ (c) Velocity errors $v_i - v_{i-1}$

(d) Positions $x_i(t)$ (e) Spacing errors $\delta_i(t)$ (f) Velocity errors $v_i - v_{i-1}$

Fig. 12. Simulation results of the 20-vehicles platoon under LBPF with the proposed method (top) and the centralized control method in [27] (bottom).

of a 20-vehicles platoon and the inter-spacing and velocity errors between neighbors. It is obviously seen that our method performs better and faster.

VI. Conclusion

In this paper, a distributed optimal platoon control framework is developed. The optimal trajectory for each following vehicle is derived in the context of distributed convex optimization based on a spacing error cost function. Then, a novel PID-type sliding mode controller with a double high-power reaching law is designed for the vehicles to track the optimal trajectory. The presented methodology can achieve smooth and stable platoon control, allowing for flexible speed regulation to guarantee steady global traffic flow.

It is worth mentioning that, the proposed framework assumes constant platoon speed (i.e., constant leader speed), which might not be the case in some situations. Then, how to optimize the leader speed to save fuel consumption and achieve compact platoon control in a distributed way? This still remains an open problem. Also, this paper assumes perfect communication and gives no hint as regards unreliable communication channels. These problems are worthy of investigation in the future.

Appendix
Proof of Theorem 1

The proof is completed by successively using the distributed optimization algorithm with time-varying cost function [28].

To prove that the reference signal $\hat{x}_i^*$ and $\hat{v}_i^*$ generated by the system (6) with $u_{i1}(t)$ is the solution of optimization problem (4a), it is only necessary to prove that the system (10) applying $u_{i1}(t)$ solves problem (11).

The lower layer of the tracking controller makes that $x_i(t) \to x_i^*(t)$ and $v_i(t) \to v_i^*(t)$ as time $t \to \infty$. So the position $x_i(t)$ and velocity $v_i(t)$ in controller (12-14) can be replaced by $x_i^*(t)$ and $v_i^*(t)$, which yields

$$\begin{aligned} u_{i1}(t) = & -\sum_{j\in I_i}\left(\eta(\hat{x}_i^*(t)-\hat{x}_j^*(t))+\tau(\hat{v}_i^*(t)-\hat{v}_j^*(t))\right) \\ & -\sum_{j\in I_i}\chi_{ij}(t)sgn(\rho(\hat{x}_i^*(t)-\hat{x}_j^*(t)) \\ & +\varsigma(\hat{v}_i^*(t)-\hat{v}_j^*(t)))+\psi_i(t) \end{aligned} \tag{38}$$

$$\dot{\chi}_{ij}(t) = \left|\rho(\hat{x}_i^*(t)-\hat{x}_j^*(t))+\varsigma(\hat{v}_i^*(t)-\hat{v}_j^*(t))\right| \tag{39}$$

$$\psi_i(t) = -2(\hat{x}_i^*(t)-\hat{x}_j^*(t))-(\hat{v}_i^*(t)-\hat{v}_j^*(t)) \tag{40}$$

First, we prove that $x_i^*(t)$ and $v_i^*(t)$ can reach consensus as $t \to \infty$.

Define $a'_{ij} = a_{ij}\chi_{ij}(t)$ and $p'_i = p_i\chi_{i0}(t)$. A new Laplacian matrix is denoted by $\mathcal{L}' = [l'_{ij}]_{N\times N}$, where $l'_{ij} = -a'_{ij}$ for $i \neq j$ and $l'_{ii} = \sum_{j=1}^{N} a'_{ij}$. The pinning matrix is $\mathcal{P}' = diag\{p'_1p'_2,\ldots,p'_N\}$. The corresponding incidence matrices are defined as $D' = [d'_{ij}]_{N\times|\mathcal{E}_N|}$ and $\bar{D}' = [d'_{ij}]_{N\times|\mathcal{E}_{N+1}|}$, respectively.

Let $\mathcal{G} = \mathcal{L}+\mathcal{P}$ and $\Theta(t) = \bar{D}'\mathrm{sgn}(\bar{D}^T(\rho\bar{X}(t)+\varsigma\bar{V}(t)))$. Define the stacked column vectors $\bar{X}(t) = [\hat{x}_1^*(t),\hat{x}_2^*(t),\ldots,\hat{x}_N^*(t)]^T$, $\bar{V}(t) = [\hat{v}_1^*(t),\hat{v}_2^*(t),\ldots,\hat{v}_N^*(t)]^T$, and $\Psi(t) = [\psi_1(t),\psi_2(t),\ldots,\psi_N(t)]^T$.

Then the closed-loop system (10) and (38) can be written in compact form

$$\begin{cases} \dot{\bar{X}}(t) = \bar{V}(t) \\ \dot{\bar{V}}(t) = -\Theta(t)+\Psi(t)-\mathcal{G}(\eta\bar{X}(t)+\tau\bar{V}(t)) \end{cases} \tag{41}$$

Utilizing the following linear transformation

$$\begin{cases} \hat{X}(t) = \Gamma\bar{X}(t) \\ \hat{V}(t) = \Gamma\bar{V}(t) \end{cases} \tag{42}$$

where matrix $\Gamma \triangleq I_N - \frac{1}{N}\mathbf{1}_N\mathbf{1}_N{}^T$, the system (41) can read as

$$\begin{cases} \dot{\hat{X}}(t) = \hat{V}(t) \\ \dot{\hat{V}}(t) = -\Theta'(t)+\Gamma\Psi(t)-\mathcal{G}(\eta\hat{X}(t)+\tau\hat{V}(t)) \end{cases} \tag{43}$$

where $\Theta'(t) = \bar{D}'\mathrm{sgn}(\bar{D}^{\mathrm{T}}(\rho\hat{X}(t)+\varsigma\hat{V}(t)))$.

Consider the Lyapunov function as follows

$$W_1(t) = \frac{1}{2}\begin{bmatrix}\hat{X}(t)\\ \hat{V}(t)\end{bmatrix}^T M\begin{bmatrix}\hat{X}(t)\\ \hat{V}(t)\end{bmatrix} + \frac{1}{4}\sum_{i=1}^{N}\sum_{j\in I_i}(\chi_{ij}(t)-\bar{\chi})^2 \tag{44}$$

where $\bar{\chi} > 0$ to be chosen and

$$M = \begin{bmatrix}(\tau\rho+\eta\varsigma)\mathcal{G} & \rho I_N \\ \rho I_N & \varsigma I_N\end{bmatrix}$$

Define matrix $\hat{M}$ as

$$\hat{M} = \begin{bmatrix}(\tau\rho+\eta\varsigma)\lambda_{\min}(\mathcal{G})I_N & \rho I_N \\ \rho I_N & \varsigma I_N\end{bmatrix}$$

It is obvious that $\hat{M} \le M$. Due to $\lambda_{\min}(\mathcal{G}) > \frac{\rho}{\tau\varsigma}$, one has

$$(\tau\rho+\eta\varsigma)\lambda_{\min}(\mathcal{G}) - \frac{\rho^2}{\varsigma} > 0$$

By Schur's complement lemma, it can be concluded that $\hat{M} \ge 0$. Then we have $0 \le \hat{M} \le M$. Therefore, M is positive definite and $W_1(t) \ge 0$.

The time derivative of $W_1(t)$ along (43) is

$$\begin{aligned} & \dot{W}_1(t) \\ & = \begin{bmatrix}\hat{X}(t)\\ \hat{V}(t)\end{bmatrix}^T M\begin{bmatrix}\hat{X}(t)\\ \hat{V}(t)\end{bmatrix} + \frac{1}{2}\sum_{i=1}^{N}\sum_{j\in I_i}(\chi_{ij}(t)-\bar{\chi})\dot{\chi}_{ij}(t) \\ & = -\rho\eta\hat{X}^T(t)\mathcal{G}\hat{X}(t)+\hat{V}^T(t)\left(\rho I_N-\tau\varsigma\mathcal{G}\right)\hat{V}(t) \\ & \quad -\frac{1}{2}\sum_{i=1}^{N}\sum_{j\in I_i}\chi_{ij}(t)\left|\rho\left(\hat{x}_i^*(t)-\hat{x}_j^*(t)\right)+\varsigma\left(\hat{v}_i^*(t)-\hat{v}_j^*(t)\right)\right| \\ & \quad +\frac{1}{N}\sum_{i=1}^{N}\sum_{j=1}^{N}\left[\rho\left(\hat{x}_i^*(t)-\hat{x}_j^*(t)\right)+\varsigma\left(\hat{v}_i^*(t)-\hat{v}_j^*(t)\right)\right]\psi_i(t) \\ & \quad +\frac{1}{2}\sum_{i=1}^{N}\sum_{j\in I_i}\left(\chi_{ij}(t)-\bar{\chi}\right)\dot{\chi}_{ij}(t) \end{aligned} \tag{45}$$

Then, suppose that $|\psi_i(t)-\psi_j(t)|$ is bounded, namely, there exists a constant $\bar{\psi}>0$ so that $|\psi_i(t)-\psi_j(t)|\leq\bar{\psi}$. It is obvious that this assumption is trivial as long as the position and speed errors of adjacent vehicles are bounded.

Since $\rho-\tau\varsigma\lambda_{\min}(\mathcal{G})<0$, then $\rho I_N-\tau\varsigma\mathcal{G}<0$ and $\hat{V}^T(t)(\rho I_N-\tau\varsigma\mathcal{G})\hat{V}(t)\leq 0$. Substituting (39) into (45), it follows from Assumption 1 and the boundness hypothesis above that

$$\begin{aligned}\dot{W}_1(t)\leq&-\rho\eta\hat{X}^T(t)\mathcal{G}\hat{X}(t)+\hat{V}^T(t)\left(\rho I_N-\tau\varsigma\mathcal{G}\right)\hat{V}(t)\\&+\left(\frac{(N-1)\,\bar{\psi}}{4}-\frac{\bar{\chi}}{2}\right)\\&\times\sum_{i=1}^{N}\sum_{j\in I_i}\left(\chi_{ij}(t)-\bar{\chi}\right)\left|\rho\left(\hat{x}_i^*(t)-\hat{x}_j^*(t)\right)\right|\\&+\left(\frac{(N-1)\,\bar{\psi}}{4}-\frac{\bar{\chi}}{2}\right)\\&\times\sum_{i=1}^{N}\sum_{j\in I_i}\left(\chi_{ij}(t)-\bar{\chi}\right)\left|\varsigma\left(\hat{v}_i^*(t)-\hat{v}_j^*(t)\right)\right|\\\leq&\left(\frac{(N-1)\bar{\psi}}{4}-\frac{\bar{\chi}}{2}\right)\left(\rho\hat{X}(t)+\varsigma\hat{V}(t)\right)^T\Theta'(t)\\\leq&\left(\frac{(N-1)\bar{\psi}}{4}-\frac{\bar{\chi}}{2}\right)\left\|\bar{D}^T\left(\rho\hat{X}(t)+\varsigma\hat{V}(t)\right)\right\|_1\\\leq&\left(\frac{(N-1)\bar{\psi}}{4}-\frac{\bar{\chi}}{2}\right)\sqrt{\lambda_{\min}(G)}\left\|\rho\hat{X}(t)+\varsigma\hat{V}(t)\right\|_2\\<&0\end{aligned}\tag{46}$$

The second inequality is derived by selecting suitable $\bar{\chi}$ which satisfy $\bar{\chi}>\frac{(N-1)\bar{\psi}}{2}$. The penultimate inequality is derived by $\mathcal{G}\triangleq\bar{D}\bar{D}^T$. With Barbalat's Lemma [29], one has that the system (43) is asymptotically stable, namely, $\hat{x}_i^*(t)=\hat{x}_j^*(t)$ and $\hat{v}_i^*(t)=\hat{v}_j^*(t)$.

The following shows that the optimization problem (11) is solved.

Consider the following Lyapunov function

$$\begin{aligned}W_2(t)=&\frac{1}{2}\sum_{i=1}^{N}\sum_{j\in I_i}\left(\hat{x}_i^*(t)-\hat{x}_j^*(t)\right)^2\\&+\frac{1}{2}\sum_{i=1}^{N}\sum_{j\in I_i}\left(\hat{x}_i^*(t)-\hat{x}_j^*(t)-\dot{v}_i^*(t)\right)^2\end{aligned}\tag{47}$$

Taking the time derivative of (47), we have

$$\begin{aligned}\dot{W}_2(t)=&\sum_{i=1}^{N}\sum_{j\in I_i}\left(\hat{x}_i^*(t)-\hat{x}_j^*(t)\right)\left(\hat{v}_i^*(t)-\hat{v}_j^*(t)\right)\\&+\sum_{i=1}^{N}\sum_{j\in I_i}\left(\hat{x}_i^*(t)-\hat{x}_j^*(t)-\dot{v}_i^*(t)\right)\left(\hat{v}_i^*(t)-\hat{v}_j^*(t)\right)\end{aligned}\tag{48}$$

Invoking $\sum_{i=1}^{N}\dot{\hat{v}}_i^*(t)=\sum_{i=1}^{N}\psi_i(t)$ and (40), we can obtain

$$\dot{W}_2(t)=\sum_{i=1}^{N}\sum_{j\in I_i}-\left(\hat{v}_i^*(t)-\hat{v}_j^*(t)\right)^2\tag{49}$$

Thus, $\dot{W}_2(t)<0$, which yields $\sum_{i=1}^{N}\sum_{j\in I_i}\left(\hat{v}_i^*(t)-\hat{v}_j^*(t)\right)$ will converge to zero asymptotically. It follows that the derivative of objective function in optimization problem (11) will approach zero. Furthermore, since the objective function is convex, it is minimized to $\hat{x}_i^*(t)$ as time goes to infinity [30]. ■

REFERENCES

[1] D. Cao *et al.*, "Future directions of intelligent vehicles: Potentials, possibilities, and perspectives," *IEEE Trans. Intell. Veh.*, vol. 7, no. 1, pp. 7–10, Mar. 2022.

[2] F.-Y. Wang, "MetaVehicles in the metaverse: Moving to a new phase for intelligent vehicles and smart mobility," *IEEE Trans. Intell. Veh.*, vol. 7, no. 1, pp. 1–5, Mar. 2022.

[3] J. Rios-Torres and A. A. Malikopoulos, "A survey on the coordination of connected and automated vehicles at intersections and merging at highway on-ramps," *IEEE Trans. Intell. Transp. Syst.*, vol. 18, no. 5, pp. 1066–1077, May 2017.

[4] G. Guo and Q. Wang, "Fuel-efficient en route speed planning and tracking control of truck platoons," *IEEE Trans. Intell. Transp. Syst.*, vol. 20, no. 8, pp. 3091–3103, Aug. 2019.

[5] S. Tsugawa, S. Jeschke, and S. E. Shladover, "A review of truck platooning projects for energy savings," *IEEE Trans. Intell. Veh.*, vol. 1, no. 1, pp. 68–77, Mar. 2016.

[6] G. Guo and S. Wen, "Communication scheduling and control of a platoon of vehicles in vanets," *IEEE Trans. Intell. Transp. Syst.*, vol. 17, no. 6, pp. 1551–1563, Jun. 2016.

[7] S. E. Li *et al.*, "Dynamical modeling and distributed control of connected and automated vehicles: Challenges and opportunities," *IEEE Intell. Transp. Syst. Mag.*, vol. 9, no. 3, pp. 46–58, Fall 2017.

[8] D. Swaroop and J. Hedrick, "String stability of interconnected systems," *IEEE Trans. Autom. Control*, vol. 41, no. 3, pp. 349–357, Mar. 1996.

[9] E. van Nunen, J. Reinders, E. Semsar-Kazerooni, and N. van de Wouw, "String stable model predictive cooperative adaptive cruise control for heterogeneous platoons," *IEEE Trans. Intell. Veh.*, vol. 4, no. 2, pp. 186–196, Jun. 2019.

[10] F. Li and Y. Wang, "Cooperative adaptive cruise control for string stable mixed traffic: Benchmark and human-centered design," *IEEE Trans. Intell. Transp. Syst.*, vol. 18, no. 12, pp. 3473–3485, Dec. 2017.

[11] S. E. Li, Y. Zheng, K. Li, and J. Wang, "An overview of vehicular platoon control under the four-component framework," in *Proc. IEEE Intell. Veh. Symp.*, 2015, pp. 286–291.

[12] P. Khound, P. Will, and F. Gronwald, "Design methodology to derive overdamped string stable asdaptive cruise control systems," *IEEE Trans. Intell. Veh.*, vol. 7, no. 1, pp. 32–44, Mar. 2022.

[13] G. Guo and D. Li, "PMP-based set-point optimization and sliding-mode control of vehicular platoons," *IEEE Trans. Computat. Social Syst.*, vol. 5, no. 2, pp. 553–562, Jun. 2018.

[14] P. Liu, A. Kurt, and U. Ozguner, "Distributed model predictive control for cooperative and flexible vehicle platooning," *IEEE Trans. Control Syst. Technol.*, vol. 27, no. 3, pp. 1115–1128, May 2019.

[15] Y. Bian *et al.*, "Fuel economy optimization for platooning vehicle swarms via distributed economic model predictive control," *IEEE Trans. Automat. Sci. Eng.*, to be published, doi: 10.1109/TASE.2021.3128920.

[16] G. J. L. Naus, R. P. A. Vugts, J. Ploeg, M. J. G. van de Molengraft, and M. Steinbuch, "String-stable CACC design and experimental validation: A frequency-domain approach," *IEEE Trans. Veh. Technol.*, vol. 59, no. 9, pp. 4268–4279, Nov. 2010.

[17] Q. Chen, Y. Zhou, S. Ahn, J. Xia, S. Li, and S. Li, "Robustly string stable longitudinal control for vehicle platoons under communication failures: A generalized extended state observer-based control approach," *IEEE Trans. Intell. Veh.*, to be published, doi: 10.1109/TIV.2022.3153472.

[18] S. Wen and G. Guo, "Distributed trajectory optimization and sliding mode control of heterogenous vehicular platoons," *IEEE Trans. Intell. Transp. Syst.*, to be published, doi: 10.1109/TITS.2021.3066688.
[19] Y. Zheng, S. E. Li, K. Li, and L.-Y. Wang, "Stability margin improvement of vehicular platoon considering undirected topology and asymmetric control," *IEEE Trans. Control Syst. Technol.*, vol. 24, no. 4, pp. 1253–1265, Jul. 2016.
[20] Y. Zheng, S. Eben Li, J. Wang, D. Cao, and K. Li, "Stability and scalability of homogeneous vehicular platoon: Study on the influence of information flow topologies," *IEEE Trans. Intell. Transp. Syst.*, vol. 17, no. 1, pp. 14–26, Jan. 2016.
[21] A. Ali, G. Garcia, and P. Martinet, "The flatbed platoon towing model for safe and dense platooning on highways," *IEEE Intell. Transp. Syst. Mag.*, vol. 7, no. 1, pp. 58–68, Spring 2015.
[22] G. Guo, P. Li, and L.-Y. Hao, "A new quadratic spacing policy and adaptive fault-tolerant platooning with actuator saturation," *IEEE Trans. Intell. Transp. Syst.*, vol. 23, no. 2, pp. 1200–1212, Feb. 2022.
[23] S. Darbha and K. Rajagopal, "Intelligent cruise control systems and traffic flow stability," *Transp. Res. Part C: Emerg. Technol.*, vol. 7, no. 6, pp. 329–352, Mar. 1999.
[24] R. Olfati-Saber and R. Murray, "Consensus problems in networks of agents with switching topology and time-delays," *IEEE Trans. Autom. Control*, vol. 49, no. 9, pp. 1520–1533, Sep. 2004.
[25] H. Sungu Emrah, M. Inoue, and J. Imura, "Nonlinear spacing policy based vehicle platoon control for local string stability and global traffic flow stability," in *Proc. Eur. Control Conf.*, 2015, pp. 3396–3401.
[26] G. Fiengo, D. G. Lui, A. Petrillo, S. Santini, and M. Tufo, "Distributed robust PID control for leader tracking in uncertain connected ground vehicles with V2V communication delay," *IEEE/ASME Trans. Mechatronics*, vol. 24, no. 3, pp. 1153–1165, Jun. 2019.
[27] C. Hossein and G. Ali, and N. Ali, "Centralized and decentralized distributed control of longitudinal vehicular platoons with non-uniform communication topology," *Asian J. Control*, vol. 21, no. 6, pp. 2691–2699, Nov. 2019.
[28] S. Rahili and W. Ren, "Distributed continuous-time convex optimization with time-varying cost functions," *IEEE Trans. Autom. Control*, vol. 62, no. 4, pp. 1590–1605, Apr. 2017.
[29] J. Slotine and W. Li, *Appl. Nonlinear Control. Upper Saddle River*, NJ, USA: Prentice-Hall, 1991.
[30] M. S. Bazaraa, H. D. Sherali, and C. M. Shetty, *Nonlinear Programming: Theory and Algorithms*. Hoboken, NJ, USA: Wiley, 2005.

Ge Guo (Senior Member, IEEE) received the B.S. and the Ph.D. degrees from Northeastern University, Shenyang, China, in 1994 and 1998, respectively.

From May 2000 to April 2005, he was with the Lanzhou University of Technology, Lanzhou, China, as a Professor and the Director of the Institute of Intelligent Control and Robots. Then he joined Dalian Maritime University, Dalian, China, as a Professor. Since 2018, he has been a Professor with Northeastern University and the Dean of the School of Control Engineering with Qinhuangdao Campus. He has authored or coauhored more than 150 international journal papers in his research field, which include intelligent transportation systems and cyber-physical systems.

Dr. Guo is an Associate Editor for the serval *IEEE Trans. ITS*, *IEEE Trans. IV*, *Information Sciences*, *IEEE ITS Magazine*, *ACTA Automatica Sinica*, *China J. Highway and Transport* and *J. Control and Decision*. He was an honoree of the New Century Excellent Talents in University, Ministry of Education, and Gansu Top Ten Excellent Youths, China. He was the recipient of the First Prize of Natural Science Award of Hebei Province and CAA Young Scientist Award.

Dongqi Yang received the B.S. degree in robot engineering from the Faculty of Robot Science and Engineering, Northeastern University, Shenyang, China, in 202, where he is currently working toward the M.E. degree in control engineering.

His research interests include intelligent transportation systems and distributed control.

Renyongkang Zhang received the B.S. degree in automation from Northeastern University, Shenyang, China, in 2020, where he is currently working the Ph.D. degree in control science and engineering with the College of Information Science and Engineering.

His research focuses on control and optimization of multiagent systems.